Model Q-II: An Underactuated Hand with Enhanced Grasping Modes and Primitives for Dexterous Manipulation

Yinkai Dong[1,2,*], Jehyeok Kim[1,*], Vatsal V. Patel[1], Huijuan Feng[2], Aaron M. Dollar[1], *Fellow, IEEE*

***Abstract*— This paper introduces Model Q-II, an enhanced underactuated robotic hand designed to improve dexterous manipulation through expanded grasping modes and manipulation primitives. The Model Q-II incorporates tripod and enhanced power grasping modes, achieving increased versatility without adding additional actuators. The design employs passive mechanisms, such as lateral contact walls and a finger-locking system, to facilitate seamless transitions between modes, enabling precise pinch-to-tripod and pinch-to-power gating. These enhancements allow the hand to perform complex in-hand manipulations, including multi-directional object positioning. Theoretical analysis, simulations, and experimental evaluations validate the hand's performance, demonstrating improved grasping force, range, and manipulation capabilities. The results highlight Model Q-II's ability to handle various tasks, offering a robust, cost-effective solution for applications requiring both precise and powerful grasping.**

I. INTRODUCTION

Enhancing the grasping modes and manipulation primitives of robotic hands is crucial for improving manipulation dexterity. A wide spectrum of modes and primitives is the main factor enabling the high dexterity of the human hand. Each manipulation mode and primitive has its own advantages and disadvantages, so implementing a range allows for the selective use of the optimal method. Numerous studies have analyzed human hand grasp taxonomies to guide robot hand development [1], [2]. These taxonomies classify various grasping modes based on object size and shape, finger positioning, and the specific requirements of power, precision, or intermediate grasps. The representative modes are pinch mode, power mode, and tripod mode. Pinch mode is ideal for precise grasping, while power mode is advantageous for increasing grasping force. The tripod mode is particularly useful for grasping irregular objects and manipulating the local position and orientation of gripped objects.

Many studies have expanded the grasping modes and primitives of robotic hands [3]–[6]. In particular, the anthropomorphic hand group has improved dexterity by actively reflecting the taxonomy of the human hand. G. Gao et al. proposed a robot hand that can switch the mode between anthropomorphic and interdigitated configuration to suit the task, achieving 5 grasping modes [7]. U. Kim et al. introduced a linkage-based compact robot hand using a total of 15 actuators [8]. This hand's high dexterity enables various modes and precise tool use by using fingertip sensors. Although these studies have successfully achieved the various modes and primitives, the high number of actuators and degrees of freedom increase their cost and control complexity.

Underactuated hands have been developed to utilize mechanical intelligence and enable robust grasping while reducing cost and controlling complexity [9]–[11]. Both intrinsic hands, which passively adapt to object shapes, and extrinsic hands, which partially adapt via external contacts, have been proposed [12]. Underactuated hands using soft materials, which can often grasp or manipulate a larger variety of objects, have also been suggested [13]. Due to compactness and easy control, these types of hands are widely used in in-

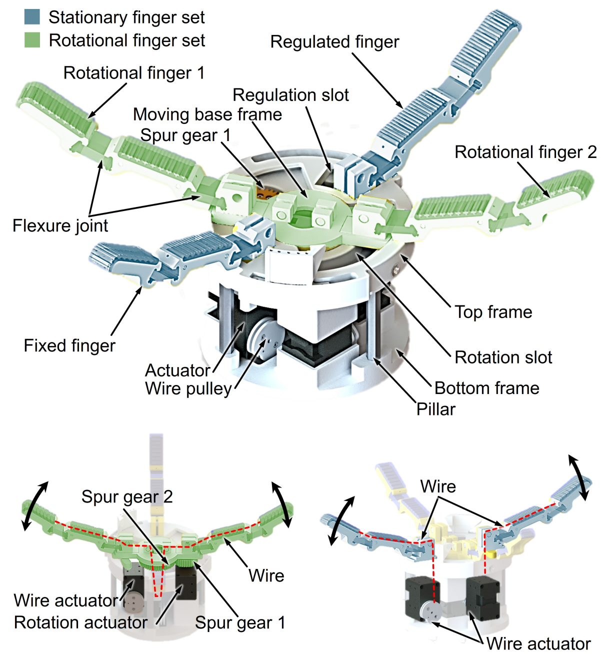

Fig. 1. Design overview of Model Q-II hand. The top illustration shows the Model Q-II hand, with four underactuated fingers and four actuators mounted on a frame base. The bottom illustration details the actuation mechanism: rotational fingers 1 and 2 are driven by a single wire actuator, while the fixed and regulated fingers are controlled by individual actuators. The rotation actuator controls the rotation of the rotational fingers through Spur gears.

This work was supported by funding from the Boston Dynamics AI Institute in Cambridge, U.S. The authors also acknowledge support from the National Natural Science Foundation of China (Grant No. 52335003), the Guangdong Basic and Applied Basic Research Foundation (Grant No. 2023A1515110644), and the Science, Technology, and Innovation Commission of Shenzhen Municipality under Grant ZDSYS20220527171403009.

*Yinkai Dong and Jehyeok Kim contributed equally to this work (co-first authors).

[1]Department of Mechanical Engineering, Yale University, CT, USA. Emails: yinkai.dong@yale.edu, jehyeok.kim@yale.edu, v.patel@yale.edu, aaron.dollar@yale.edu

[2]Shenzhen Key Laboratory of Intelligent Robotics and Flexible Manufacturing Systems, Southern University of Science and Technology, Shenzhen 518055, China, fenghj@sustech.edu.cn

dustrial applications. However, because underactuated hands rely on few actuators, they are limited in their dexterous manipulation capabilities.

To overcome low dexterity, researchers have developed underactuated hands with multiple modes. D. Chappel et al. introduced a hand that can change the grasping mode by reconfiguring the base position of the finger, resulting in pinch, partial power, and quadpod modes [14]. Partial power mode refers to a mode in which two fingers are located on the same plane so that it fails to grasp relatively small objects due to collision between the fingertips. Likewise, a new hand developed for the ANA Avatar XPRIZE Challenge shows that adding compliant elements for everyday tasks can simplify the design [15]. In [16], the SARAH hand achieved pinch, power, and tripod modes by rotating the angle of the finger base, but it focused only on grasping and did not address improving dexterity through manipulation primitives. Ma et al. proposed the hand Model Q, which greatly improved the modes and primitives of underactuated hands [17]. The Model Q has a fixed set of fingers and a rotating set of fingers. Through this configuration, pinch, partial power, and quadpod modes were achieved, and three further primitives were implemented: pinch-to-power gating, continuous in-hand twisting, and finger pivoting. A.S. Morgan et al. showed that Model Q successfully enabled complex in-hand manipulation [18]. However, Model Q still has the disadvantage of not being able to use tripod mode and power grasping mode.

In this study, our goal is to enhance the grasping modes and manipulation primitives based on Model Q, aiming to achieve higher dexterity in robotic hands. Here, we propose Model Q-II that is not only equipped with the modes and manipulation primitives of Model Q, but also achieves enhanced power mode and tripod mode simultaneously. Furthermore, Model Q-II has additional manipulation primitives, including pinch to tripod, pinch to power, and tripod manipulation. These enhancements are acquired without additional actuators. In power-grasp mode, Model Q-II reduces the minimum graspable diameter from 94.1 mm to 50.8 mm, demonstrating a 46% improvement and significantly increased the maximum grasping force. In addition, the workspace of in-hand manipulation of tripod mode, which Model Q cannot implement, is analyzed by a preliminary experiment.

This paper is structured as follows. Section II explains the mechanism design of Model Q-II. The manipulation capabilities are presented in Section III. In Section IV, the theoretical force analysis model and its results are addressed. Experimental validation of the additional grasping modes is explained in Section V.

II. Hand Mechanism Design

A. Design overview

The Model Q-II expands upon the design of the Model Q hand, which performs pinch, partial power, and quadpod grasping modes. By inheriting these core functionalities and incorporating additional grasping modes—tripod grasping and an enhanced power grasping mode—the Model Q-II significantly elevates its versatility and adaptability in complex manipulation tasks. To understand the overall structure of Model Q-II, a comprehensive view of the hand is shown in Fig. 1.

The Model Q-II consists of a top frame, a bottom frame, four actuators, and four underactuated fingers. The actuators are positioned between the bottom frame and the top frame, driving the fingers via pulley systems. The four fingers are classified into the stationary and rotational finger sets. The stationary set includes a fixed finger and a regulated finger and the rotational set includes rotational fingers 1 and 2. The fixed finger is anchored to the top frame, providing a stable reference point that supports the other fingers during grasping operations. The regulated finger, which can be moved within a regulation slot, is key to determining the grasping mode. The passive movement of the regulated finger is triggered when it is contacted by the rotational finger 2 through its respective finger base, causing the regulated finger to rotate within the slot. A compression spring, as shown in Fig. 2(a), is installed in the regulation slot allows the finger to return to its original position once the contact is removed. The fixed and regulated fingers are driven by their own wire actuators, enabling precise control of their positioning. The rotational fingers 1 and 2 are mounted on a moving base, allowing them to move freely within the rotation slot. The rotation actuator rotates the moving base frame through the spur gears 1 and 2. Unlike the stationary finger set, the rotational fingers are driven by one shared wire actuator. Additionally, once the actuator cable is relaxed, the elasticity of the flexure joints restores the finger to its open configuration.

B. Tripod grasping mode

Fig. 2(a) illustrates the tripod mode mechanism of Model Q-II. In tripod mode, the rotational finger set can occupy one of two key positions: state 1 and state 2.

State 1 is the default alignment, where the wire stopper is not blocked by any wall, and both rotational fingers (1 and 2) move freely with the actuator's pull. State 2 is triggered when the rotational base rotates counterclockwise and brings the wire stopper into contact with the stop wall. In this position, the motion of rotational finger 2 is locked out, allowing independent actuation of rotational finger 1.

When the rotational finger set is in state 1, the shared wire for rotational fingers 1 and 2 is pulled without obstruction. Moving the finger set into state 2 activates the wire stopping mechanism; the wire stopper meets the stop wall, preventing rotational finger 2 from closing further while finger 1 remains actively driven through the floating pulley. Meanwhile, rotational finger 1 pushes the base of the regulated finger, shifting it out of the plane of the fixed finger so that these three fingers (fixed, regulated, and rotational finger 1) form a stable tripod around the object. This extra contact point allows additional degrees of freedom for in-plane and out-of-plane manipulations, distinguishing tripod mode from simpler pinch or quadpod grasping mode.

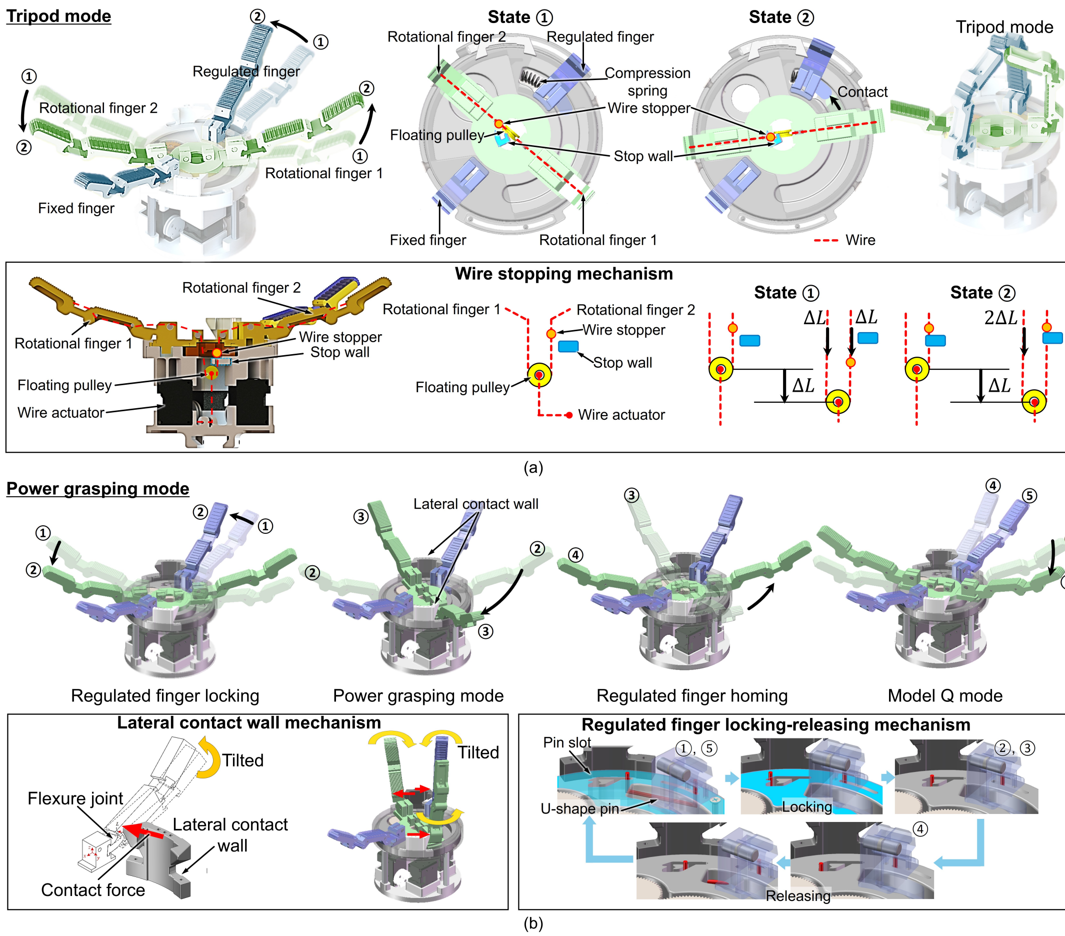

Fig. 2. Configuration and operating concepts of Model Q-II hand. (a) The tripod grasping mode forms a triangular grip with three fingers. Rotational finger 1 pushes the regulated finger from state 1 to 2 through the contact block, moving the wire stopper into the stop wall. This allows the actuator to control rotational finger 1 independently. (b) The power grasping mode interdigitates the rotational and fixed fingers. The locking-releasing mechanism locks the regulated finger when pushed by the rotational finger 1. The lateral contact wall mechanism adjusts the orientation of the rotational and regulated fingers to enable interdigitation.

C. Power grasping mode

Power grasping mode is achieved through a lateral contact wall mechanism and a regulated finger locking releasing mechanism as shown in Fig. 2(b). Since the joints of each finger are composed of flexure joints, the fingers can be tilted when lateral force is applied to the side surface of the fingers. When the fingers are tilted, the gripping motion does not occur in the same plane, allowing interdigitation between the fingertips, which enables enhanced power gripping. First, rotational finger 1 moves counterclockwise and strongly presses the regulated finger through the finger base element. The moved regulated finger tilts due to contact with the upper lateral wall fixed to the top frame. Next, the rotational finger set rotates clockwise. This clockwise rotation makes rotational finger 2 contact the upper lateral wall and rotational finger 1 contact the lower lateral wall, resulting in the tilt of both fingers. As a result, these three fingers form a configuration that enables power grasping mode.

Since a compression spring is installed in the regulation slot, when the contact between rotational finger 1 and the regulated finger disappears, the regulated finger must be restored to its original position. To prevent this, Model Q-II is equipped with a finger-locking-releasing mechanism. The U-shaped pin engages the pin slot when the regulated finger is pressed, preventing spring-driven restoration. The lateral walls guide the pin in place. Once the rotational finger repositions, the pin is released, allowing the regulated finger to return to its original position.

By strategically controlling finger positions, the power grasping mode enables the Model Q-II to achieve a robust and stable grasp configuration suited for high-force tasks.

D. Fabrication and assembly

The Model Q-II was fabricated based on detailed design specifications derived from simulations. Structural components—including the base and fingers—were printed using polylactic acid (PLA) filament for its ease of printing and sufficient strength for prototyping. To achieve the necessary compliance in the joints, flexure joints were created using PMC-780, a polyurethane rubber molded directly onto the 3D-printed finger structures. Finger pads were cast using Dragon Skin 30 silicone rubber to enhance grip and prevent slippage during object manipulation. The final assembly involved integrating the fabricated fingers with the actuation system, consisting of four Dynamixel XM430-W210-R servomotors mounted between the top frame and the bottom frame. A tendon-driven mechanism was implemented using high-strength, low-stretch cables routed through pulleys and guides within the fingers and base.

III. Enhanced Manipulation Capabilities

A. Grasping modes

The grasping modes of Model Q-II, inherited from Model Q, are pinch mode using two fingers and quadpod mode, as shown in Figure 3(a) and (b), respectively. The objects used in the grasping experiments cover a weight range of approximately 50 g to 400 g and a size range of 4 cm to 20 cm in their longest dimension. Although Model Q is also capable of a power grasping mode, due to physical interference between the fingertips, it can only be used to grasp relatively large objects. Figure 3(c) illustrates the enhanced power grasping mode of Model Q-II. This mode allows power grasping of smaller objects. Finally, the tripod mode of Model Q-II is represented in Figure 3(d). This proposed robotic hand can grasp irregularly shaped objects through tripod mode.

B. Manipulation primitives

Model Q-II basically achieves manipulation primitives inherited from Model Q, which consists of pinch-to-partial power, in-hand twisting, and finger-pivoting manipulation. In pinch-to-partial power primitive, the object initially grasped in pinch mode is moved toward the palm by continuous caging motion to improve grasping stability. As shown in Fig. 4(a), the finger pivoting manipulation is used to rotate an object, with one set of fingers holding it while another set of fingers rotating it. This rotation is generated around a virtual axis formed by the two fingers holding the object. In-hand twisting manipulation is a mode that allows the hand to continuously rotate the object by the rotation function of the rotational finger base and repetitive changes in the grasping finger set, as shown in Fig. 4(b). These two manipulation primitives are essential for changing the orientation of the gripped object.

Additional achieved manipulation primitives are pinch-to-tripod, pinch-to-enhanced power and tripod in-hand manipulation. In pinch-to-tripod manipulation, the fixed and regulated fingers are initially used to grip an object, as shown in Fig. 4(c). To switch to tripod mode, the rotational finger base rotates to push the regulated finger base to form a tripod configuration. Then, a rotational finger is quickly moved to contact with the gripped object. This primitive, which connects the two grasping modes, is crucial for enabling the continuous execution of complex manipulation tasks. Fig. 4(d) illustrates the pinch-to-enhanced power manipulation primitive. Initially, the hand uses the two rotational fingers to perform a precise pinch grasp. To transition to the power grasping phase, the rotational finger base is rotated to position the gripped object properly. Next, the gripped object is gently released from the pinch grasp in the air. The object settles into the palm area, and then the fixed and regulated fingers envelop the object securely. This process allows Model Q-II to start with precision handling and seamlessly shift to a strong, stable grip. Tripod in-hand manipulation is performed by controlling the fixed finger, the regulated finger and the rotational finger 1. This primitive is useful when delicate position and orientation manipulation of a gripped object is required, as illustrated in Section V.

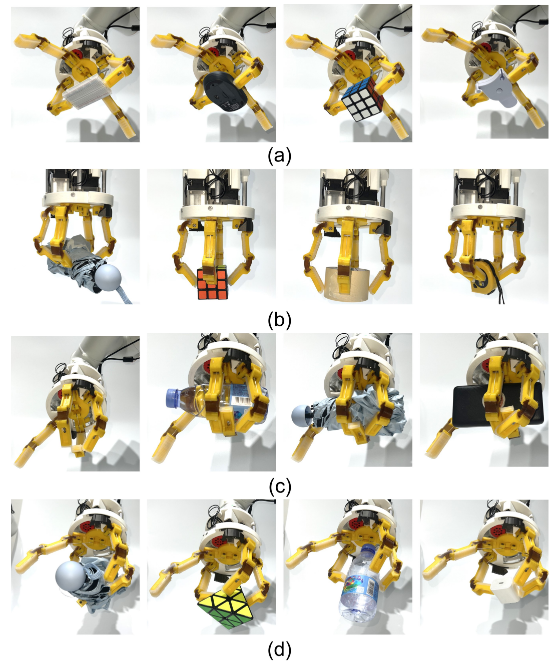

Fig. 3. Grasping experiments of the Model Q-II hand with objects of various shapes and sizes. (a) Pinch grasping mode. (b) Quadpod grasping mode. (c) Power grasping mode. (d) Tripod grasping mode.

IV. Force Analysis

A. Statics analysis of Model Q-II finger

The Model Q-II enhances gripping performance and flexibility through a structure comprising a finger base, proximal joint, proximal phalanx, distal joint, and distal phalanx. To evaluate the stability and grasping capabilities, we developed a mathematical model capturing key mechanical properties. The positioning of the finger segments follows:

$$\mathbf{r}_{i+1} = \mathbf{r}_i + l_{i+1} \cdot \mathbf{n}_{i+1} \tag{1}$$

where $\mathbf{r}_i$ is the position vector of the i-th key point, l_{i+1} is the length of the segment, and $\mathbf{n}_{i+1}$ is the directional unit vector. This relation reflects the sequential arrangement of the finger from base to tip, providing the kinematic foundation.

The equilibrium between the torque input, joint stiffness of proximal and distal joints (k_1, k_2), related joint angle, and the contact force at the distal joint is expressed as:

$$\mathbf{F} \cdot l_F = \mathbf{M}\left(\tau_{input}, \mathbf{r}_i\right) - \sum\nolimits_{m=1}^{2} k_m \theta_m \tag{2}$$

In this equation, τ_{input} denotes the actuator torque, k_m represents the stiffness of the m-th joint, and θ_m is the bending angle. This relation links the actuator torque to the resulting

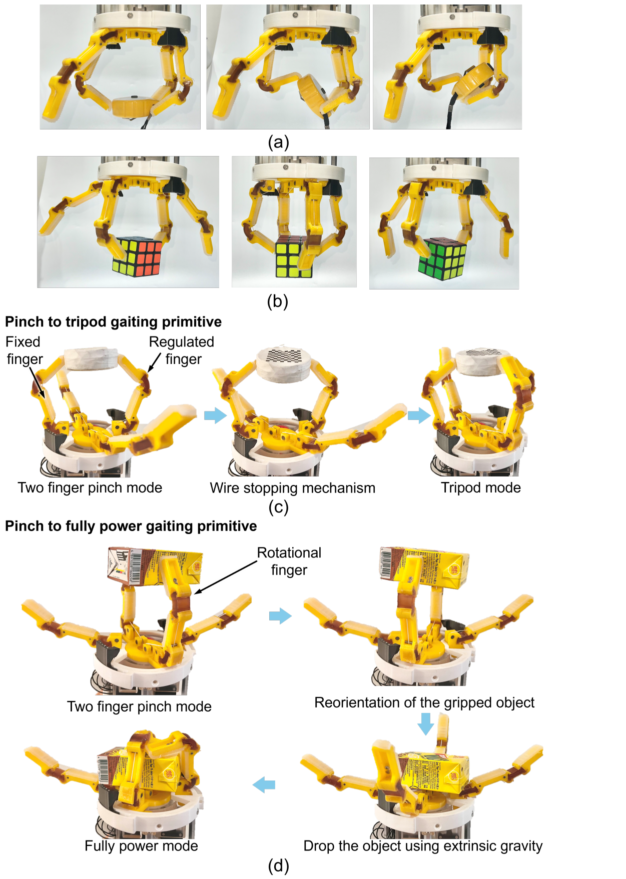

Fig. 4. Manipulation of the Model Q-II hand with distinct grasping modes and mode combinations: (a) Finger-pivoting primitive, (b) In-hand twisting primitive, (c) Pinch-to-tripod primitive, (d) Pinch-to-enhanced power primitive.

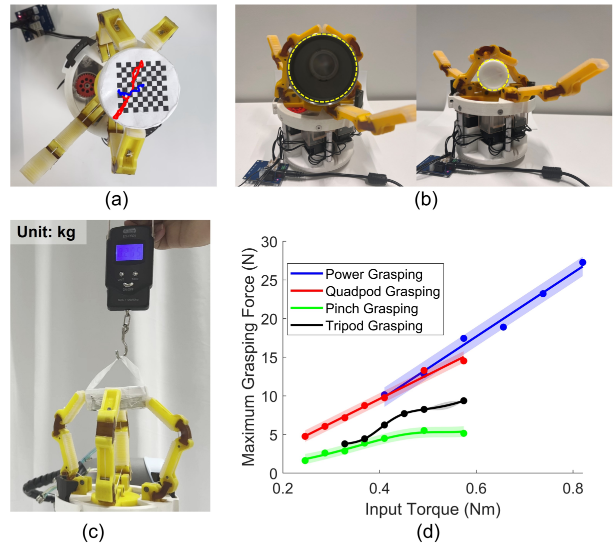

Fig. 5. (a) Tripod manipulation with trajectory tracking at the object's center; red points show forward and backward manipulation, while the blue line indicates lateral manipulation. (b) Grasping range validation for quadpod two-finger power grasp (minimum diameter: 94.1 mm) and interdigitated power grasp (minimum diameter: 54.8 mm). (c) Experiment setup for maximum force measurement. (d) Maximum grasping force at varying input torques across different grasping modes.

forces within the hand by accounting for both the geometry and the elastic properties of the flexure joints, providing insights into how the applied torque translates into gripping forces.

The bending angles of the proximal and distal joints, 1 and 2, are obtained through numerical methods. The relationship governing these angles is represented by:

$$\theta_{1,j+1}, \theta_{2,j+1} = f\left(\tau_{\text{input}}, \mathbf{r}_i\left(\theta_{1,j+1}, \theta_{2,j+1}\right), \ldots\right) \quad (j = 1, 2, \ldots) \tag{3}$$

This equation describes how the angles evolve based on input torques and current joint positions, requiring iterative numerical methods for precise calculation.

B. Contact force simulation of Model Q-II finger

Fig. 5 presents the simulation results of the contact forces at the distal phalanx with the rotation edge when the input torque is 0.4 N·m. The red line in Fig. 5 represents the workspace boundary of the proximal and distal joints. This boundary was determined by numerically solving the Equation (3) relating the bending angles with the applied actuator torque and the stiffness of the flexure joints.

Common household objects, like a 200 g soda can, typically require 5–10 N of normal force to prevent slipping. Based on this, our analysis assumes a 10 N clamping force per side for stability. Analysis of Fig. 5(a) and (b) shows that the contact force in the X direction is positive in 86.48% of grasping scenarios, with forces exceeding 10 N in 61.70% of cases, contributing to a stable grasp. The Z direction force is negative in 80.03% of the workspace, crucial for object retention, and the Y direction force is negative in 80.03% of cases, with values below -10 N in 53.92%, enhancing downward stability. The optimal region for pinch grasps (pinch, quadpod, tripod) occurs where $F_x > 10$ N and $F_z < 0$, representing 44.23% of the workspace. For power grasps, characterized by stronger engagement, the effective region is where $F_z < 10$, covering 53.92% of the workspace. These findings highlight the Model Q-II finger's adaptability, effectively utilizing flexure joints to perform both precision and power grasps.

Overall, the simulation confirms the significant flexibility and grasping capabilities of the Model Q-II finger, demonstrating that controlled input torque enhances stability and efficiency across various grasping scenarios.

V. Experimental Evaluation

A. Tripod manipulation

In tripod mode, the Model Q-II significantly expands its manipulation capabilities beyond what is achievable with the Model Q hand. While Model Q allows manipulation primarily along the grasping direction, similar to pinch manipulation, Model Q-II goes further. It enables in-plane manipulation along the finger grasping direction and also facilitates out-of-plane manipulation, including lateral adjustments that are impossible with the Model Q. The experimental results from Fig. 6(a) show that the range for forward manipulation is 60.18 mm, while the range for lateral

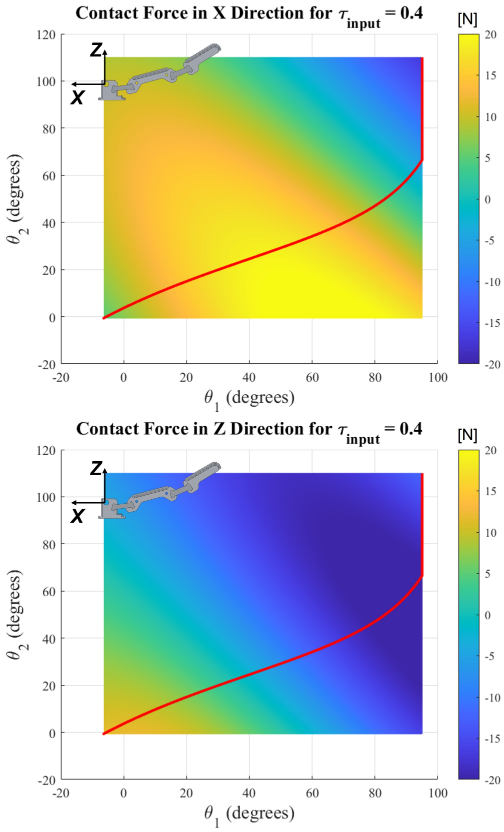

Fig. 6. Simulation results of contact forces at the distal phalanx relative to joint angles at the proximal (θ_1) and distal (θ_2) joints in the (a) X direction and (b) Z direction. The range above the red line in the figure is the grasping workspace of the Model Q-II hand.

manipulation is 26.96 mm, highlighting the enhanced spatial flexibility of the Model Q-II.

B. Power grasping range identification

In partial power grasping mode, which is the same as that of Model Q, the minimum diameter for grasping is 94.1 mm. However, Model Q-II significantly reduces this minimum diameter to 50.8 mm, achieving a reduction of approximately 46% by the enhanced power grasping mode, as shown in Fig. 6(b). The limitation in power grasping mode arises when the distal phalanges of the opposing pinch fingers come into contact with each other, preventing further closure and restricting the grasp size. In contrast, Model Q-II overcomes this issue through interdigitation, allowing the fingers to pass between each other, thus enabling a tighter grasp.

C. Grasping force measurement

Figures 6(c) and 6(d) show the experimental setup and results for maximum grasping force across different modes. The experiment assessed the performance of the Q-II model hand in four grasping modes. For pinch, tripod and quadpod modes, the hand grasped a cylindrical object of 6.25 cm diameter, 3.8 cm height under varying input torques. A force gauge applied a vertical pull to measure the maximum force maintaining a stable grasp, with tests repeated five times. For power grasping mode, the force gauge applied a lateral force to assess grasp robustness, keeping all other setup conditions constant. The results show that in the tripod mode, the stabilizing force distribution lies between those of the pinch and power modes. This demonstrates that tripod mode offers a balanced grasping force, combining elements of precision and stability. For power grasping, an object with a 72 mm diameter—below the minimum size for partial power grasping—was used. The proposed hand utilized interdigitation to grasp the object, and force was applied laterally to the hand with varying torque inputs. The force distribution in the enhanced power mode was found to be higher than that of the partial power mode.

These findings indicate that Model Q-II expands the graspable range in tripod mode and enhances grasping force, especially in enhanced power mode. The ability to interdigitate allows the hand to handle smaller objects with increased stability and force, demonstrating its superior performance compared to traditional hand configurations.

VI. Conclusion

This paper presented the design, analysis, implementation, and experimental evaluation of Model Q-II, an enhanced underactuated robotic hand with multifunctional capabilities for advanced manipulation. Building upon the Model Q design, the Model Q-II incorporates additional grasping modes—tripod and enhanced power grasping—greatly increasing its versatility in complex tasks. The hand design features passive mechanisms for seamless mode transitions, allowing the hand to dynamically adapt its grasp during operation, such as shifting from pinch to power grasping. This is achieved through mechanisms like the lateral contact wall and finger-locking-releasing system, enabling smooth transitions without additional actuators.

Static analysis and simulations characterized the hand's mechanical properties, providing detailed insights into its workspace, grasping forces, and rotational performance. Experimental evaluations validated its performance across all four basic grasping modes: pinch, quadpod, tripod, and power grasping. Compared to the Model Q, the Model Q-II demonstrated significant improvements. Notably, in power grasping mode, the Model Q-II reduced the minimum graspable object diameter by approximately 46%, allowing it to securely grip smaller objects that were previously unattainable. Additionally, in tripod mode, the Model Q-II enabled manipulation of a gripped object in the grasping direction and laterally, offering enhanced versatility. Specifically, the hand achieved a manipulation range of 60.18 mm in the forward direction and 26.96 mm laterally—capabilities that the Model Q could not provide. These enhancements highlight the superior performance of the Model Q-II over its predecessor, expanding its manipulation capabilities and applicability in more complex tasks. Future work will optimize design and control strategies, explore advanced materials, integrate tactile sensors, and conduct extensive real-world testing to further enhance versatility. The design files and documentation for Model Q-II will be open-sourced through the Yale OpenHand project [19].

REFERENCES

[1] M. R. Cutkosky *et al.*, "On grasp choice, grasp models, and the design of hands for manufacturing tasks." *IEEE Transactions on robotics and automation*, vol. 5, no. 3, pp. 269–279, 1989.

[2] T. Feix, J. Romero, H.-B. Schmiedmayer, A. M. Dollar, and D. Kragic, "The grasp taxonomy of human grasp types," *IEEE Transactions on human-machine systems*, vol. 46, no. 1, pp. 66–77, 2015.

[3] L. B. Bridgwater, C. Ihrke, M. A. Diftler, M. E. Abdallah, N. A. Radford, J. Rogers, S. Yayathi, R. S. Askew, and D. M. Linn, "The robonaut 2 hand-designed to do work with tools," in *2012 IEEE International Conference on Robotics and Automation*. IEEE, 2012, pp. 3425–3430.

[4] E. Emmanouil, G. Wei, and J. S. Dai, "Spherical trigonometry constrained kinematics for a dexterous robotic hand with an articulated palm," *Robotica*, vol. 34, no. 12, pp. 2788–2805, 2016.

[5] G. Li, X. Liang, Y. Gao, T. Su, Z. Liu, and Z.-G. Hou, "A linkage-driven underactuated robotic hand for adaptive grasping and in-hand manipulation," *IEEE Transactions on Automation Science and Engineering*, 2023.

[6] L. Kang, Y. Yang, J. Yang, and B.-J. Yi, "A three-fingered adaptive gripper with multiple grasping modes," in *2021 IEEE/RSJ International Conference on Intelligent Robots and Systems (IROS)*. IEEE, 2021, pp. 6097–6103.

[7] G. Gao, J. Chapman, S. Matsunaga, T. Mariyama, B. MacDonald, and M. Liarokapis, "A dexterous, reconfigurable, adaptive robot hand combining anthropomorphic and interdigitated configurations," in *2021 IEEE/RSJ International Conference on Intelligent Robots and Systems (IROS)*. IEEE, 2021, pp. 7209–7215.

[8] U. Kim, D. Jung, H. Jeong, J. Park, H.-M. Jung, J. Cheong, H. R. Choi, H. Do, and C. Park, "Integrated linkage-driven dexterous anthropomorphic robotic hand," *Nature communications*, vol. 12, no. 1, pp. 1–13, 2021.

[9] T. Laliberte, L. Birglen, and C. Gosselin, "Underactuation in robotic grasping hands," *Machine Intelligence & Robotic Control*, vol. 4, no. 3, pp. 1–11, 2002.

[10] L. U. Odhner, L. P. Jentoft, M. R. Claffee, N. Corson, Y. Tenzer, R. R. Ma, M. Buehler, R. Kohout, R. D. Howe, and A. M. Dollar, "A compliant, underactuated hand for robust manipulation," *The International Journal of Robotics Research*, vol. 33, no. 5, pp. 736–752, 2014.

[11] H. Isakhani, S. Nefti-Meziani, S. Davis, and H. Isakhani, "A bioinspired underactuated dual tendon-based adaptive gripper for space applications," in *2023 IEEE/RSJ International Conference on Intelligent Robots and Systems (IROS)*. IEEE, 2023, pp. 2447–2454.

[12] H. Hua, Z. Liao, and J. Zhao, "Design, analysis, and experiment of an underactuated robotic gripper actuated by linear series elastic actuator," *Journal of Mechanisms and Robotics*, vol. 15, no. 2, p. 021002, 2023.

[13] J. Shintake, V. Cacucciolo, D. Floreano, and H. Shea, "Soft robotic grippers," *Advanced materials*, vol. 30, no. 29, p. 1707035, 2018.

[14] D. Chappell, F. Bello, P. Kormushev, and N. Rojas, "The hydra hand: A mode-switching underactuated gripper with precision and power grasping modes," *IEEE Robotics and Automation Letters*, 2023.

[15] E. Sung, S. You, S. Kim, and J. Park, "Snu-avatar robot hand: Dexterous robot hand with prismatic four-bar linkage for versatile daily applications," in *2023 IEEE-RAS 22nd International Conference on Humanoid Robots (Humanoids)*, 2023, pp. 1–8.

[16] C. M. Gosselin and T. Laliberte, "Underactuated mechanical finger with return actuation," Jun. 9 1998, uS Patent 5,762,390.

[17] R. R. Ma and A. M. Dollar, "An underactuated hand for efficient finger-gaiting-based dexterous manipulation," in *2014 IEEE International Conference on Robotics and Biomimetics (ROBIO 2014)*. IEEE, 2014, pp. 2214–2219.

[18] A. S. Morgan, K. Hang, B. Wen, K. Bekris, and A. M. Dollar, "Complex in-hand manipulation via compliance-enabled finger gaiting and multi-modal planning," *IEEE Robotics and Automation Letters*, vol. 7, no. 2, pp. 4821–4828, 2022.

[19] R. Ma and A. Dollar, "Yale openhand project: Optimizing open-source hand designs for ease of fabrication and adoption," *IEEE Robotics & Automation Magazine*, vol. 24, no. 1, pp. 32–40, 2017.